

# A Fairness-based Performance Evaluation of Fractional Frequency Reuse in LTE

Josep Colom Ikuno, Martin Taranetz, Markus Rupp

Institute of Telecommunications

Vienna University of Technology, Austria

Gusshausstrasse 25/389, A-1040 Vienna, Austria

Email: {jcolom, martin.taranetz, mrupp}@nt.tuwien.ac.at

Web: <http://www.nt.tuwien.ac.at/ltesimulator>

**Abstract**—This paper evaluates the downlink performance of Fractional Frequency Reuse (FFR) in Long Term Evolution (LTE) networks employing a metric combining throughput and fairness, which we argue better depicts the effects of FFR. This is as opposed to previous work, which focused on capacity-based metrics, evaluating only the mean, peak (95%), and edge (5%) points of the capacity distribution. We evaluate FFR on a multi-user setup combined with round robin and proportional fair scheduling in a hexagonal grid scenario. We conclude that, compared to traditional scheduling, FFR does not provide tangible gains.

## I. INTRODUCTION

Fractional Frequency Reuse (FFR) is based on dividing the cell area into a center part, named the Full Reuse (FR) zone, where interference is lower and reuse-1 is employed, and an outer part, named the Partial Reuse (PR) zone, where a higher frequency reuse factor is employed, as shown in Figure 1 for the case of a PR reuse factor of three. Thus, this co-channel interference mitigation scheme aims at combining the high spectral efficiency at cell center of a reuse-one scheme and the better (compared to reuse-one) spectral efficiency of higher-reuse schemes.

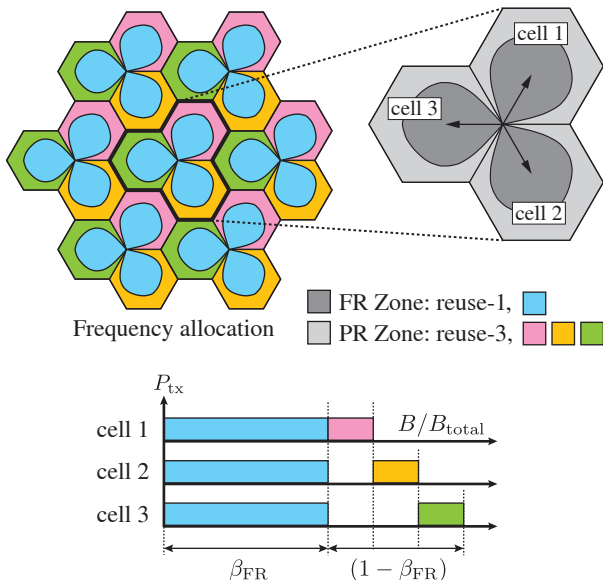


Fig. 1. FFR frequency partitioning of a sectorized cell.

The fractional frequency partitioning is accomplished by assigning a fraction  $\beta_{FR}$  of the total available bandwidth to the FR zones, while the remaining fraction  $(1 - \beta_{FR})$  employs a reuse- $n$  scheme. In this work we consider reuse-3 in the PR zone), as shown on Figure 1.

FFR performance is typically assessed in literature by means of three Key Performance Indicators (KPIs). These KPIs, which are derived from the throughput empirical cdf (ecdf) and do not take into account the effects of scheduling [2–9], consist of: (i) mean throughput, (ii) edge throughput, and (iii) peak throughput. The terms “edge” and “peak” refer, as widely employed in literature, to the 5% and 95% points of the User Equipment (UE) throughput ecdf, respectively. These can be interpreted as the performance of a UE at the cell edge and at cell center, respectively.

However, just looking at these KPIs, skewed distributions with seemingly all-improving results could be misinterpreted as favorable results. Such a distribution could be easily caused by an FFR configuration in which most of the throughput is served to a handful of users which would then be making up for most of the mean. Simultaneously a majority of users would experience reduced throughput, which albeit low, could be significantly higher than the original reuse-1 5% percentile.

## II. PRIOR WORK

In previous work [10], we argued that capacity is not a suitable metric for FFR partitioning, as capacity does not capture the fact that the Physical (PHY) resources the FR/PR zones are distributed over the attached UEs and not assigned to a single UE. Instead, we proposed a capacity density metric, which is analogous to throughput assuming (i) that each UE is attached to the reuse zone where it would achieve a higher throughput (FR or PR), (ii) and assuming a homogeneous UE distribution and PHY resource allocation.

Denoting as  $\rho$  the points  $(x, y)$  separating the FR and PR areas and as  $\beta_{FR}$  the ratio of the bandwidth dedicated to FR (each PR gets 1/3 of the remaining), the capacity density  $c$  is expressed as

$$c_{FFR, \rho, \beta_{FR}}(x, y) = \begin{cases} c_{FR, \rho, \beta_{FR}}(x, y) & \text{if } (x, y) \in \text{FR} \\ c_{PR, \rho, \beta_{FR}}(x, y) & \text{if } (x, y) \in \text{PR} \end{cases}, \quad (1)$$

where the capacity densities for the FR and PR zones for a position  $(x, y)$  given a FR-PR boundary  $(\rho)$  and FFR bandwidth partitioning  $(\beta_{FR})$  are a function of the Shannon capacity at  $(x, y)$ :

$$c_{FR,\rho,\beta_{FR}}(x, y) = \frac{\beta_{FR}}{A_{FR}(\rho)} \log_2(1 + \Gamma_{FR}(x, y)) \quad (2)$$

$$c_{PR,\rho,\beta_{FR}}(x, y) = \frac{1 - \beta_{FR}}{3 A_{PR}(\rho)} \log_2(1 + \Gamma_{PR}(x, y)), \quad (3)$$

where for both the FR and PR zones, and indicated by the corresponding subscript,  $\Gamma$  denotes the SINR at position  $(x, y)$ , and  $A$  denotes the area of the zone. The partition boundary  $\rho$  is chosen such that  $c_{FR,\rho,\beta_{FR}}(\rho) = c_{PR,\rho,\beta_{FR}}(\rho)$ . Thus, and as shown in [10],  $c_{FFR}$  becomes a function of just  $\beta_{FR}$  and  $(x, y)$ .

In [10], we maximized the average capacity density, denoted as  $\bar{c}$  formulating the following optimization problem:

$$\max_{\beta_{FR}} \bar{c}_{FFR}(\beta_{FR}) \quad (4)$$

$$\text{subject to } 0 \leq \beta_{FR} \leq 1 \quad (5)$$

$$c_{5\%,FFR} \geq c_{5\%,reuse1}, \quad (6)$$

which aims at maximizing the mean capacity density constrained to no loss of edge capacity density (denoted as  $c_{5\%,FFR}$ ) with respect to the reuse-1 case ( $c_{5\%,reuse1}$ ). The results, which were obtained considering the same hexagonal cell setup as in this paper (see Section III), are shown on Figure 2.

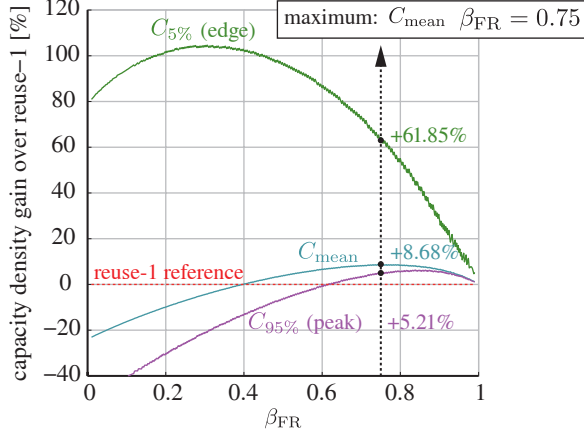


Fig. 2. FFR mean, edge, and peak capacity density gains relative to reuse-1, as found on [10]. A sectorized hexagonal grid with an  $8^\circ$  electrical tilt is considered.

### III. THROUGHPUT-AND-FAIRNESS-BASED METRIC AND EMPLOYED SYSTEM MODEL

In order to evaluate performance in terms of throughput, the Vienna LTE system level simulator [11] has been extended to support FFR. Simulations employing both round robin and proportional fair scheduling have been carried out.

The round robin simulations provide a scenario analogous to that in [10], where capacity density is employed through an assumption of a constant UE density and equal UE PHY

resource allocation, which is the allocation performed by a round robin scheduler. The proportional fair simulations are, on the contrary, aimed at evaluating whether any potential gains with proportional fair scheduling are also present with a more realistically-employed scheduling algorithm. In both cases, an independent scheduler is employed for the FR and PR zones, effectively having two schedulers per cell.

We used a hexagonal grid layout and employed the simulation parameters listed in Table I. Note that shadow fading was omitted in order to be able to characterize the cell boundary  $\rho$  by means of an SINR threshold  $\Gamma_{thr}$ , resulting in a layout similar to that depicted on Figure 1<sup>1</sup>.

TABLE I  
SIMULATION PARAMETERS EMPLOYED FOR THE LTE FFR SIMULATIONS.

Inter-eNodeB distance	500 m [13]
Number of eNodeBs	57 (two rings, 19 sites). Only 21 inner cells taken into account for the results.
UEs per eNodeB	30
Considered UEs	Center 7 sites (21 cells): 630 UEs
Transmission bandwidth	20 MHz (100 Resource Blocks)
Antennas ( $N_{TX} \times N_{RX}$ )	$4 \times 4$
MIMO mode	CLSM [14]
Feedback	AMC: CQI, MIMO: PMI and RI
Feedback delay	3 ms
Channel model	Winner Phase II [15, 16]
UE speed	5 km/h
Receiver model	Zero Forcing [11]
Noise spectral density	-174 dBm/Hz
Pathloss model	Urban area [12], 70 dB MCL [12]
Shadow fading	none
Minimum coupling loss	70 dB [12]
Antenna pattern	KATHREIN 742212
Antenna downtilt	$8^\circ$ , electrical
TX power	40 W
Simulation length	50 subframes (TTIs)
Traffic model	Full buffer
Scheduling algorithm	Round Robin and Proportional fair [17]
$\Gamma_{thr}$ range	-2:0.25:22.5 (99 values)
$\beta_{FR}$ range	0.01:0.03:1 (34 values)

As in LTE the total transmission bandwidth is partitioned in individually-schedulable units of 180 kHz, termed Resource Blocks (RBs), the employed values for  $\beta_{FR}$  range between 0.01 and 1, with a 0.03 step, representing a range between 1 and 100 LTE RBs. The SINR threshold  $\Gamma_{thr}$  ranges from -2 dB and 22.5 dB (a 0.25 dB step is considered), which represent the extreme values found on the cell. For each of the two scheduling algorithms, this yields a total of 3 366 FFR configurations being tested, each one of which is evaluated by means of a system level simulation.

The initial intention aimed at showing whether the gains seen in the capacity density-based results directly applied to throughput. However, after application of the link abstraction model and a more detailed review of the throughput distribution of the UE results, it was realized that throughput

<sup>1</sup>The employed antenna pattern (KATHREIN 742212) has been extensively used in our simulations to depict a more realistic pattern than those in [12]. Although it could have changed for a newer pattern corresponding to an XX-Pol panel, for consistency, it is also used in this context, although it corresponds to an XX-Pol panel.

distributions such as those shown on Figure 3 are common when applying FFR. These skewed distributions, although good if only the traditional KPIs are taken into account, are however not desired in network deployments, as mentioned in Section I

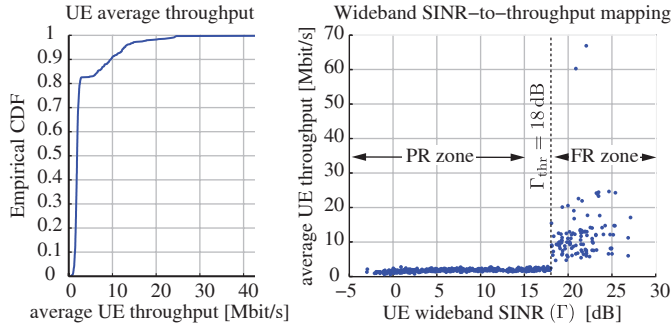


Fig. 3. UE throughput distribution for ( $\beta_{\text{FR}} = 0.31, \Gamma_{\text{thr}} = 18$  dB). Left: UE throughput ecdf. Right: UE throughput over wideband SINR ( $\Gamma$ ). According to the throughput KPIs, overall gain is obtained, despite the obvious undesirable distribution: Mean UE throughput of 3.66 Mbit/s (+11.15% compared to reuse-1), edge throughput of 1.28 Mbit/s (+73.04%), and peak throughput of 12.91 Mbit/s (+75.28%).

In this paper we propose, as previously mentioned, that a performance metric combining throughput and fairness allows for a better performance evaluation of FFR.

Fairness rates how equally a resource (in this case throughput) is distributed over  $N$  users, and is defined in [18] as

$$J(\mathbf{x}) = \frac{\left(\sum_{i=1}^N x_i\right)^2}{N \sum_{i=1}^N x_i^2}, \quad (7)$$

where  $\mathbf{x}$  is a vector of length  $N$ , containing the throughput obtained by each of the  $N$  users. Graphically, a fairness of one would be visualized on the results in Figure 3 as a throughput ecdf with a pendent of one and a flat SINR-to-throughput plot, while a minimum fairness would produce a step function ecdf and a single non-zero throughput point in the SINR-to-throughput plot.

#### IV. SIMULATION RESULTS

In this section, simulation-based results are presented. For each scheduling algorithm, range of  $\beta_{\text{FR}}$  and  $\Gamma_{\text{thr}}$  values listed in Table I has been simulated, taking as performance metrics the mean UE throughput, edge UE throughput, peak UE throughput, and fairness.

Among the complete set of FFR configurations, the region where the obtained FFR fairness (denoted as  $J_{\text{FFR}}$ ) is bigger or equal than that obtained with reuse-1 (denoted as  $J_{\text{reuse1}}$ ) is considered.

In sections IV-A and IV-B, the simulation results for the round robin and proportional case scheduling scenarios, respectively, are detailed.

##### A. Round Robin Results

Figure 4 depicts the simulation results for the round robin scheduling scenario, where results are shown over the  $\beta_{\text{FR}}$  range (x-axis) and the  $\Gamma_{\text{thr}}$  (y-axis).

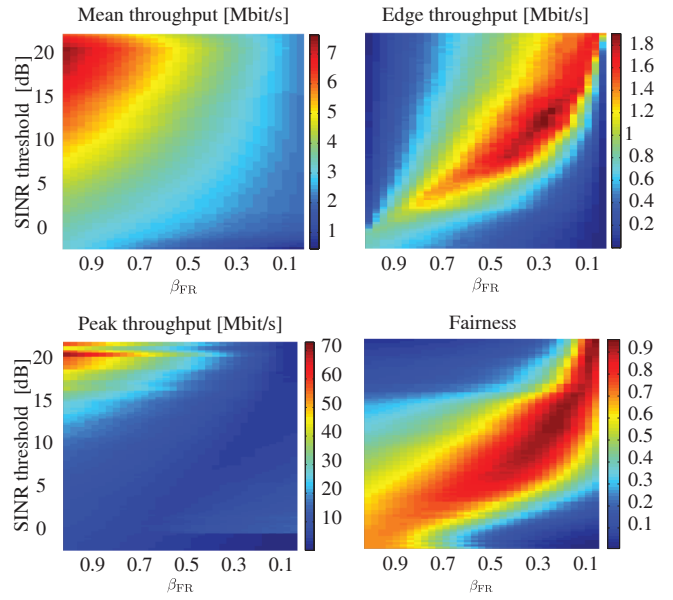


Fig. 4. FFR results with round robin scheduling. Top-left: mean UE throughput. Top-right: edge UE throughput. Bottom-left: peak UE throughput. Bottom-right: fairness..

For each of the  $(\beta_{\text{FR}}, \Gamma_{\text{thr}})$ , each of the points depicted in the plots represents, from left to right and top to bottom, the mean, edge, peak, and fairness result for the corresponding FFR configuration. For each case, the upper-rightmost corner represent a reuse-3-equivalent setup ( $\beta_{\text{FR}} = 0$  and  $\Gamma_{\text{thr}}$  set up so as to assign the whole area to the PR zone), while the lower-leftmost corner represents a reuse-1-equivalent setup ( $\beta_{\text{FR}} = 1$  and  $\Gamma_{\text{thr}}$  set up so that the FR zone spans the whole cell).

The considered results set is constrained to the FFR configurations where  $J_{\text{FFR}} \geq J_{\text{reuse1}}$ , for which we want to evaluate the trade-off between mean throughput gain and fairness. For this purpose, a graphical representation such as that in Figure 5 is more suitable.

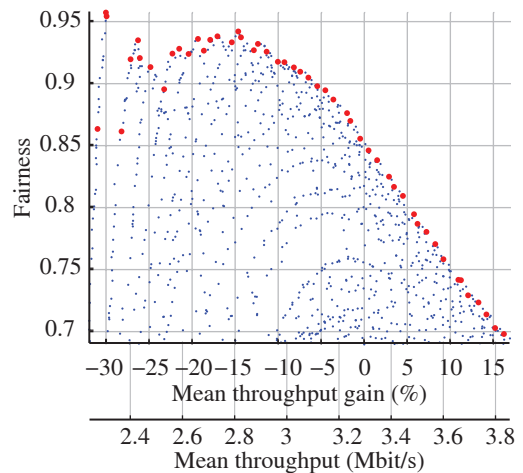


Fig. 5. Round robin scheduling trade-off between fairness and mean UE throughput. Marked red are the optimum mean-throughput-to-fairness trade-off FFR configurations.

In Figure 5, each of the points in the scatterplot depicts the mean throughput and fairness of an FFR configuration for which a fairness higher than that of reuse-1 has been achieved. Constraining  $J_{\text{FFR}} \geq J_{\text{reuse1}}$  ensures that throughput is spread among users at least as equally as in the reuse-1 case, and thus avoids skewed distributions.

The red dots mark the optimum mean-throughput-to-fairness trade-off FFR configurations, i.e., the points where fairness is maximum relative to the throughput gain.

An equivalent depiction of the edge and peak UE throughput results is shown in Figure 6.

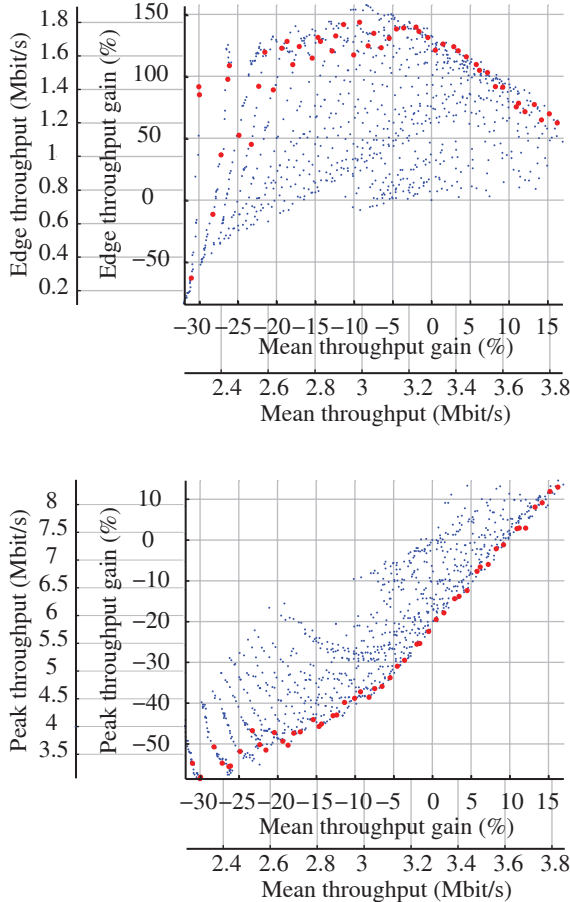


Fig. 6. Round robin scheduling edge (top) and peak (bottom) throughput vs. mean UE throughput for the FFR configurations where a fairness gain is achieved. The marked dots correspond to the same marked configurations in Figure 5.

Also for the FFR configurations where  $J_{\text{FFR}} \geq J_{\text{reuse1}}$ , edge (top) and peak (bottom) UE throughput are plotted against mean throughput loss. Marked red are the same optimum mean-throughput-to-fairness trade-off points marked in Figure 5, thus showing the edge and peak throughput performance of the FFR configurations of interest.

The results depicted in Figures 5 and 6 show that, by means of applying FFR, it is possible to: (i) improve mean (+16.2%), edge (+62.4%), and peak (+13%) throughput without a fairness loss, thus proving the main point in [10], and (ii) achieve maximum optimum fairness-to-mean-throughput trade-off which

improves fairness to 0.94 at the cost of a 14% loss in mean throughput, a 131% gain in edge throughput, and a 45% loss in peak throughput.

However, round robin scheduling is known to be Pareto sub-optimal [19]. It achieves lower throughput and fairness compared to more optimal scheduling algorithms such as proportional fair [17, 20, 21], which are hence more commonly used.

### B. Proportional Fair Results

In this subsection we consider the more realistically-employed proportional fair scheduler, and apply the same evaluation methodology shown in Section IV-A to this scenario.

In Figure 7, the relation between fairness and mean throughput for the proportional fair case is shown. While similar in shape to the round robin results in Figure 5, the throughput values indicate that FFR cannot increase fairness without sacrificing mean throughput.

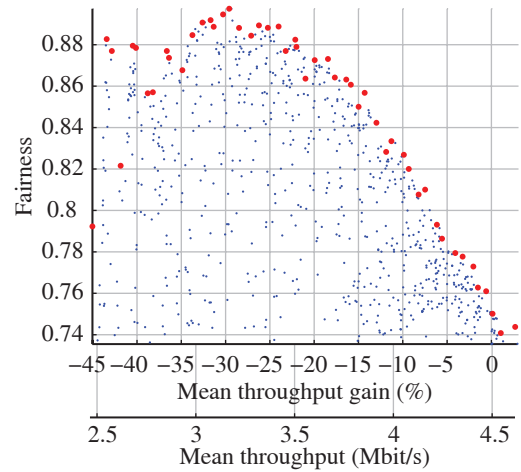


Fig. 7. Proportional fair scheduling trade-off between fairness and mean UE throughput. Marked red are the optimum mean-throughput-to-fairness trade-off FFR configurations.

While in the round robin case, up to a 16% gain in mean UE throughput could be achieved without reducing fairness, the relative gains seen in the rightmost part of Figure 7 indicate that is not able improve mean throughput over the reuse-1 case in this fairness-constrained case ( $J_{\text{FFR}} \geq J_{\text{reuse1}}$ ).

A similar behavior is observed of the relation between edge and peak UE throughput and mean UE throughput shown in Figure 8.

As opposed to the round robin case, the results in Figure 8 show that a fairness optimization does invariably imply a reduction in peak throughput (bottom plot). Additionally edge throughput gains (top plot) are more difficult to extract, as seen from the range of FFR configurations with edge throughput gain compared to the round robin case.

From the simulation results, it is concluded that, when applied on top of proportional fair scheduling, FFR *cannot* introduce a gain in average throughput if fairness is to be maintained.

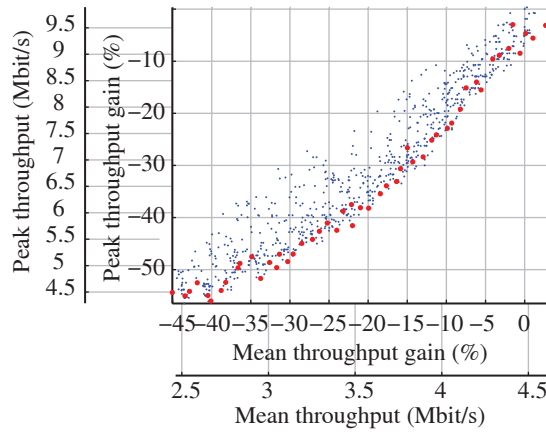
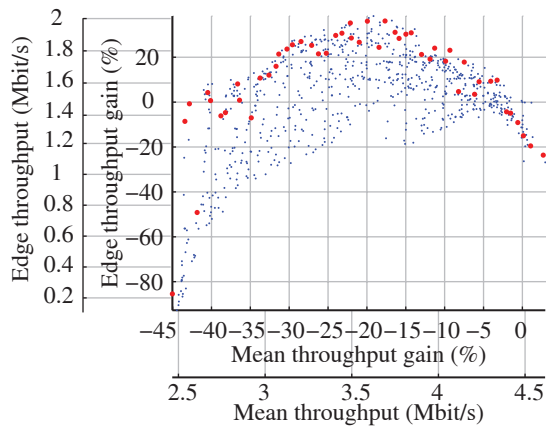


Fig. 8. Proportional fair scheduling edge (top) and peak (bottom) throughput vs. mean UE throughput for the FFR configurations where a fairness gain is achieved. The marked dots correspond to the same marked configurations in Figure 7.

### C. FFR Performance gain

The combined results of round robin and proportional fair scheduling are shown in Figure 9. For each of the scheduling algorithms, the plot depicts the envelope marked in Figures 5 and 7. Results show that, unless a fairness is to be completely prioritized independent of throughput degradation ( $J > 0.9$ ), proportional fair always outperforms round robin.

As seen from the results shown in Figure 9, FFR can increase the throughput without decreasing fairness only in the case of round robin scheduling, although the gain vanishes if it is employed on top of proportional fair scheduling. However, tweaking the FFR parameters does allow for a flexible trade-off between fairness and throughput. Two operating points of interest for network deployments have been evaluated: (i) maximum mean throughput without fairness loss, and (ii) maximum achievable fairness while maintaining an optimum mean-throughput-to-fairness trade-off, which are marked in Figures 9–11 as (i) and (ii), respectively.

In Figures 10 and 11, analogous plots are shown for the relationship of the mean UE throughput vs. edge and peak UE throughput, respectively. As expected from the relationship

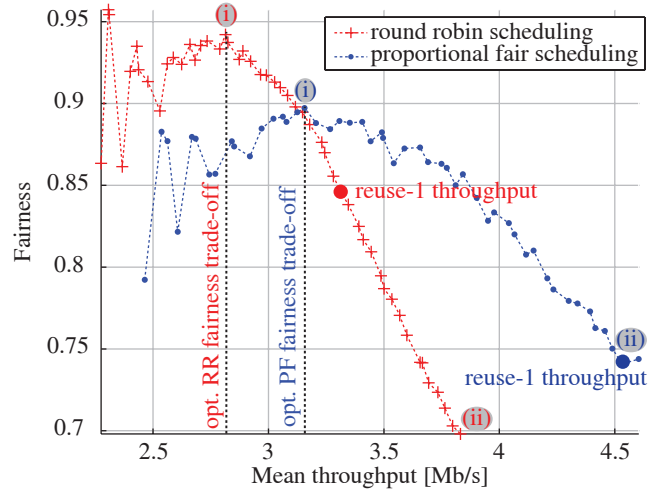


Fig. 9. Fairness trade-off over mean UE throughput: round robin and proportional fair scheduling.

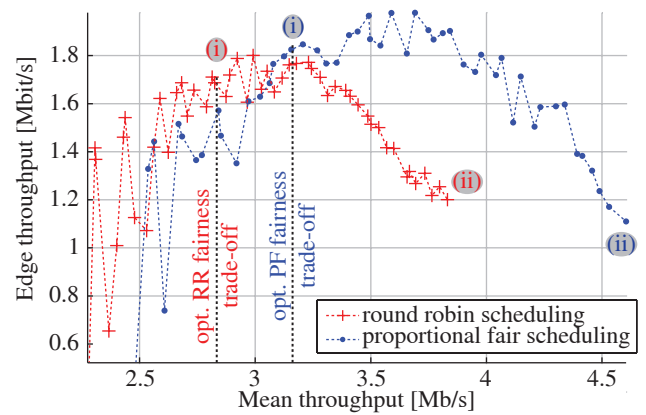


Fig. 10. Edge UE throughput vs. mean UE throughput: round robin and proportional fair scheduling.

imposed between mean, edge, and peak throughput by the fairness constraint, the same effects seen in Figure 9 are seen in Figures 10 and 11.

The most desirable situation would be that of a “free” gain also for the proportional fair scheduler, where the throughput accomplished in target (i) is higher than that of the reuse-1 case or when in (ii), higher fairness values can be achieved without decreasing throughput. However, as seen from the results in Figures 9–11, this is *not* possible.

## V. CONCLUSIONS

In this paper we evaluate FFR performance when applied to LTE networks. We employ a combined metric taking into account throughput and fairness, which aims at a more suitable metric than prior capacity-based ones. Scenarios combining FFR with two different scheduling algorithms (round robin and proportional fair) have been considered, employing in both case a hexagonal cell layout. Results show that if the fairness of the UE throughput distribution is to be maintained, FFR offers no gain if proper scheduling is employed.

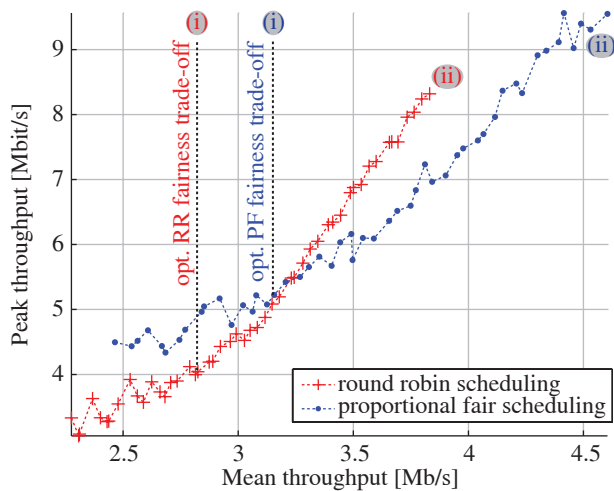


Fig. 11. Peak UE throughput vs. mean UE throughput: round robin and proportional fair scheduling.

All data, tools and scripts will be available online in order to allow other researchers to reproduce our results [1].

#### ACKNOWLEDGMENTS

The authors would like to thank the LTE research group for continuous support and lively discussions. This work has been funded by the Christian Doppler Laboratory for Wireless Technologies for Sustainable Mobility, KATHREIN-Werke KG, and A1 Telekom Austria AG. The financial support by the Federal Ministry of Economy, Family and Youth and the National Foundation for Research, Technology and Development is gratefully acknowledged.

#### REFERENCES

- [1] "LTE link and system level simulator download site." [Online]. Available: <http://www.nt.tuwien.ac.at/ltesimulator/>
- [2] T. Novlan, J. Andrews, I. Sohn, R. Ganti, and A. Ghosh, "Comparison of fractional frequency reuse approaches in the OFDMA cellular downlink," in *Proceedings of the 2010 IEEE Global Telecommunications Conference (GLOBECOM2010)*, Baltimore, Maryland, Dec. 2010.
- [3] M. Assaad, "Optimal fractional frequency reuse (FFR) in multicellular OFDMA system," in *IEEE 68th Vehicular Technology Conference (VTC2008-Fall)*, Calgary, Canada, Sep. 2008.
- [4] M. Rahman and H. Yanikomeroglu, "Enhancing cell-edge performance: a downlink dynamic interference avoidance scheme with inter-cell coordination," *IEEE Transactions of Wireless Communications*, vol. 9, no. 4, pp. 1414–1425, Apr. 2010.

- [5] A. Najjar, N. Hamdi, and A. Bouallegue, "Efficient frequency reuse scheme for multi-cell OFDMA systems," in *IEEE Symposium on Computers and Communications (ISCC2009)*, Sousse, Tunisia, Jul. 2009.
- [6] V. Jungnickel, M. Schellmann, L. Thiele, T. Wirth, T. Haustein, O. Koch, W. Zirwas, and E. Schulz, "Interference-aware scheduling in the multiuser MIMO-OFDM downlink," *IEEE Communications Magazine*, vol. 47, no. 6, pp. 56–66, Jun. 2009.
- [7] Z. Xie and B. Walke, "Frequency reuse techniques for attaining both coverage and high spectral efficiency in ofdma cellular systems," in *IEEE Wireless Communications and Networking Conference (WCNC2010)*, Sydney, Australia, Apr. 2010.
- [8] A. Simonsson, "Frequency reuse and intercell interference co-ordination in e-utra," in *IEEE 65th Vehicular Technology Conference (VTC2007-Spring)*, Dublin, Ireland, Apr. 2007.
- [9] L. Chen and D. Yuan, "Generalized frequency reuse schemes for OFDMA networks: Optimization and comparison," in *IEEE 71st Vehicular Technology Conference (VTC2010-Spring)*, Taipei, Taiwan, May 2010.
- [10] M. Taranetz and J. C. Ikuno, "Capacity density optimization by fractional frequency partitioning," in *45th Annual Asilomar Conference on Signals, Systems, and Computers (ASILOMAR2011)*, Pacific Grove, California, Nov. 2011.
- [11] J. C. Ikuno, M. Wrulich, and M. Rupp, "System level simulation of LTE networks," in *71st Vehicular Technology Conference (VTC2010-Spring)*, Taipei, Taiwan, May 2010.
- [12] Technical Specification Group Radio Access Network, "E-UTRA; LTE RF system scenarios," 3GPP, Tech. Rep. TR 36.942, Dec. 2008.
- [13] —, "E-UTRA; further advancements for E-UTRA physical layer aspects," 3GPP, Tech. Rep. TR 36.814, Mar. 2010.
- [14] —, "E-UTRA; physical channels and modulation," 3GPP, Tech. Rep. TS 36.211, May 2009.
- [15] Members of WINNER, "Assessment of advanced beamforming and MIMO technologies," WINNER, Tech. Rep. IST-2003-507581, 2005.
- [16] L. Hentilä, P. Kyösti, M. Käske, M. Narandzic, and M. Alatossava, "MATLAB implementation of the WINNER phase ii channel model ver1.1," Dec. 2007. [Online]. Available: [http://www.ist-winner.org/phase\\_2\\_model.html](http://www.ist-winner.org/phase_2_model.html)
- [17] Z. Sun, C. Yin, and G. Yue, "Reduced-complexity proportional fair scheduling for OFDMA systems," in *2006 International Conference on Communications, Circuits and Systems (ICCCAS2006)*, Guilin, China, Jun. 2006.
- [18] R. K. Jain, D.-M. W. Chiu, and W. R. Hawe, "A Quantitative Measure Of Fairness And Discrimination For Resource Allocation In Shared Computer Systems," Digital Equipment Corporation, Tech. Rep., Sep. 1984.
- [19] S. Schwarz, C. Mehlhruher, and M. Rupp, "Throughput maximizing multiuser scheduling with adjustable fairness," in *IEEE International Conference on Communications (ICC2011)*, Kyoto, Japan, Jun. 2011.
- [20] A. Jalali, R. Padovani, and R. Pankaj, "Data throughput of CDMA-HDR a high efficiency-high data rate personal communication wireless system," in *IEEE 51st Vehicular Technology (VTC2000-Spring)*, Tokyo, Japan, 2000.
- [21] S. Schwarz, J. Colom Ikuno, M. Šimko, M. Taranetz, Q. Wang, and M. Rupp, "Pushing the Limits of LTE: A Survey on Research Enhancing the Standard," *arXiv e-prints*, Dec. 2012.